STATIC LOADING TESTS AND A COMPUTATIONAL MODEL OF A FLEXIBLE NET

Jun FUJIWARA[1], Shinya SEGAWA[1], Kenshi ODA[1], Fumio FUJII[2], Makoto OHSAKI[3], Hirohisa NOGUCHI[4]

[1] *Research Engineer, Advanced Structures R&D Dept., Taiyo Kogyo Corp., 3-20, Shodai-tajika, Hirakata-shi, Osaka, 573-1132, Japan*

[2] *Professor, Dept. of Mathematical and Computational Engineering, Gifu Univ., Gifu 501-1193, Japan*

[3] *Assoc. Professor, Dept. of Architecture and Architectural Engineering, Kyoto Univ., Nishikyo-ku, Kyoto 615-8540, Japan*

[4] *Professor, Dept. of System Design Engineering, Keio Univ., 3-14-1, Hiyoshi, Kohoku-ku, Yokohama 223-5822, Japan*

E-mail: fj003177@mb.taiyokogyo.co.jp, ss000971@mb.taiyokogyo.co.jp, ok000408@mb.taiyokogyo.co.jp, ff@cc.gifu-u.ac.jp, ohsaki@archi.kyoto-u.ac.jp, noguchi@sd.keio.ac.jp

ABSTRACT

In the field of architectural engineering, highly pre-stressed cable nets are used for supporting lightweight roof structures. In contrast to these highly pre-stressed nets, low- or non-tensioned nets, for example sports nets, spider nets, hammocks, fishing nets and mosquito nets, are frequently observed in our living and natural environments. In this paper, these nets are called *flexible nets*. Because of low pre-stresses, large scale of sag can be observed in even a state where only dead loads are applied. When practical loads are applied, flexible nets may extremely deform. Furthermore computational operations may be complicated, since these nets can transmit only tensile stresses. Therefore, flexible nets have been rarely adapted to architectural engineering. To the authors' knowledge, only a few experimental and computational studies have been published on this particular type of flexible nets. In this paper, static loading tests are performed on a flexible net that has hexagonal unit. Numerical analyses are also carried out.

1 INTRODUCTION

Highly pre-stressed cable nets are widely applied for architectural roof structures. Since introduced pre-stresses give stiffness to structures and cancel compressive stresses due to external loads, lightweight and stiff structures can be realized. Several studies have been published and some applications can be observed[1-12].

On the other hand, in contract to these highly pre-stressed nets, low- or non-tensioned nets are frequently used in our living and natural environments. Sports nets, spider nets, hammocks, fishing nets are examples. Because of its extreme flexibility, shape of low- or non-tensioned nets can dramatically change due to external loads. The deformation also strongly depends on the boundary condition. In this paper, these extremely flexible nets are called *flexible nets*.

Because many flexible nets are made with lightweight fiber, for examples nylon and polyester, and pre-stresses are significantly low, it is easy to attach and remove from given boundary. Furthermore, flexible nets have permeability with respect to not only light but also air and water. As stated above, flexible nets have unique characteristics, compared with general architectural materials that are used for tension structures, and further applications in engineering field are expected.

To the authors' knowledge, however, only a few experimental and computational studies have been published on this particular type of flexible nets. Followings may be considered as reasons why flexible nets have not been regarded as a subject of engineering study.

1. From the viewpoint of measuring technique, it is difficult to measure configuration, stress and strain, accurately, because flexible nets are extremely sensitive to inperfection.
2. From the computational viewpoint, since net segments can transmit only tensile stresses, stiffness matrix can be singular in computational process.

In this paper, static loading tests are performed on an extremely flexible net that has hexagonal unit. Numerical analyses are also carried out. The experimental and computational results are compared for verifying the accuracy of the computational model. The static response characteristic of the flexible net are also discussed.

2 LOADING TESTS AND COMPUTATIONAL MODEL

2.1 Configuration in non-stressed state

A polyester net is submitted to the loading tests. As shown in Figure 1, the net is clamped to a 2180 mm × 2180 mm square boundary frame. The net has hexagonal units and consists of two kinds of segment. The thick segments are parallel to the arrow direction in Figure 1, and a pair of thin segment is twisted to form one thick segment.

In the case where a flexible net has multiple degrees of freedom in kinematic mechanism motion, it is difficult to define the configuration in non-stressed state. In this study, the net is put on a flat floor and fixed in a 2180 mm × 2180 mm square (shown in Figure 2). Since the self-weight of the net is canceled in the state where the net is on the flat floor, the state can be considered as non-stressed state. The configuration of the net and length of the segments are measured. In the numerical analyses, the measured configuration is given as the initial state where the strains of all segments are equal to zero. A segment is modeled as a finite element[13-15]. The initial shape of computational model and the dimensions of the hexagonal unit are indicated in Figures 3 (a) and (b). The Z-axis is supposed to be normal to the X-Y plane.

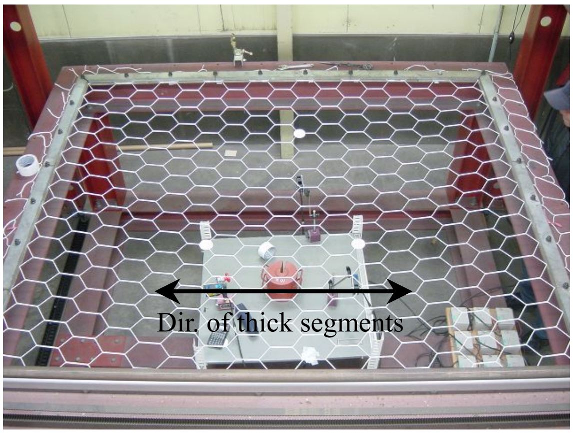

Figure 1. A net clamped to a boundary frame

Figure 2. A net on a flat floor

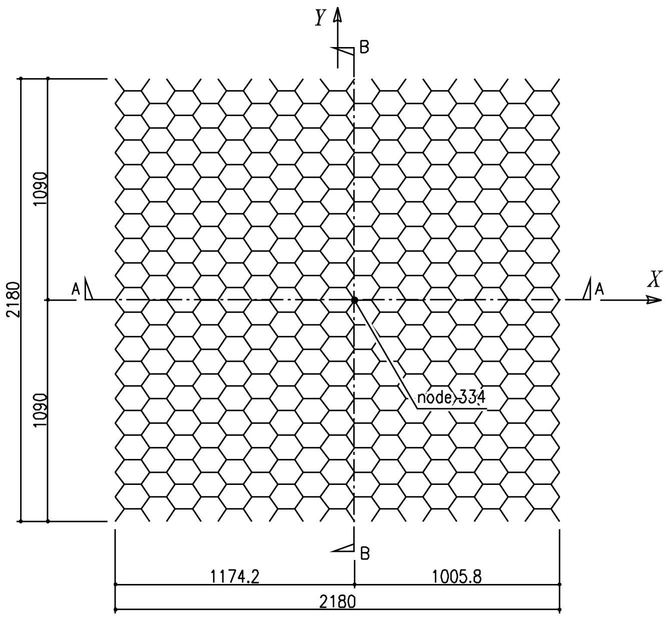

(a) Plan

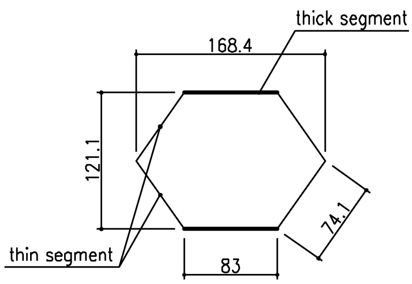

(b) A hexagonal unit

Figure 3. A computational model and node number (unit: mm)

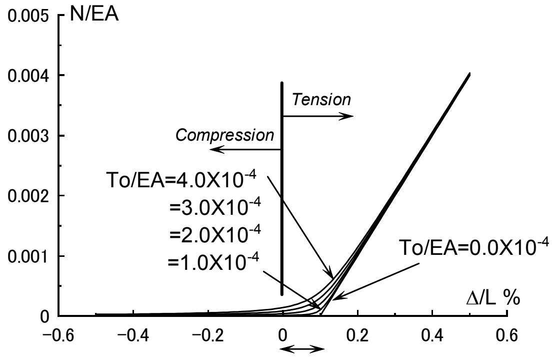

Figure 4. Modeled stress-strain relationship of a segment

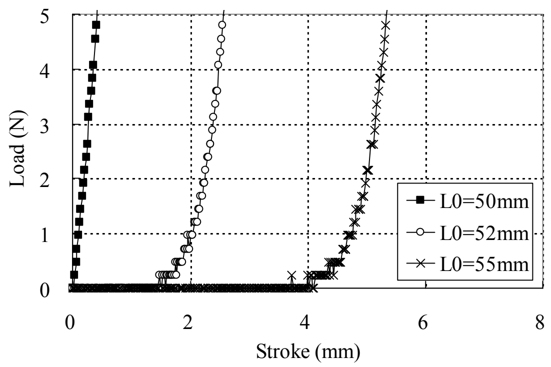

(a) Thin segment

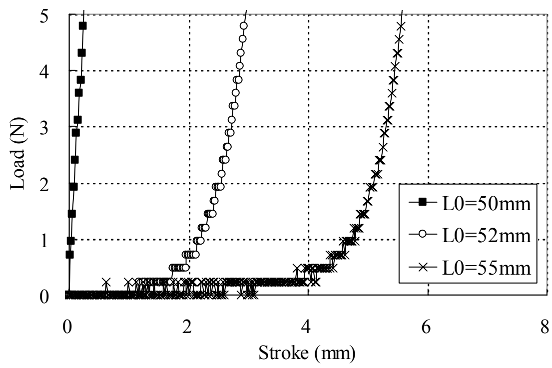

(b) Thick segment

Figure 5. Load-stroke relations of net segments

2.2 Constitutive laws of net segments

It is assumed that the net segments do not have compressive or bending stiffness. Let N, Δ, EA and L denote the axial force, elongation, axial stiffness and initial length of the segment, respectively. The relation between N and Δ is given as

$$\frac{N}{EA} = \frac{1}{2}\left\{\left(\frac{\Delta}{L} - \varepsilon_0\right) + \sqrt{\left(\frac{\Delta}{L} - \varepsilon_0\right)^2 + 4\left(\frac{T_0}{EA}\right)^2}\right\} \tag{1}$$

where ε_0 and T_0 are the initial slackness and axial force when Δ/L is equal to ε_0, respectively. The stress-strain relationship based on (1) is as shown in Figure 4. In Figure 4, five kinds of value of T_0/EA, 4.0×10^{-4}, 3.0×10^{-4}, 2.0×10^{-4}, 1.0×10^{-4} and 0.0×10^{-4}, are considered. If T_0 is equal to 0.0, as shown in Figure 4, a bi-linear type stress-strain relationship is given, and the stiffness is discontinuous at $\Delta/L = \varepsilon_0$. Therefore, iteration in equilibrium analysis is stabilized by giving a small value to T_0.

The values of EA, ε_0 and T_0 are obtained based on tensile tests of net segments. In the tests, the initial distance of chucks and tensile speed are 50 mm and 0.2 mm/min, respectively. Length of the segments L_0 is parametrically changed: $L_0 = 50$, 52 and 55 mm. The results of the thin and thick segments are shown in Figures 5 (a) and (b). The filled squares, blank circles and crosses represent $L_0 = 50$, 52 and 55, respectively. The obtained material parameters of the thin and thick segments are listed in Table 1, where M denotes the mass of segment. The load-stroke relations based on (1) and the tests are shown in Figures 6 (a) and (b), where the blank circles and solid lines indicate the experimental and computational results, respectively.

Table 1. Material parameters

	Thin segment	Thick segment
L (mm)	74.1	83.0
EA (N)	560	200
ε_0	0.0003	0.02
T_0 (N)	0.01	0.7
M (g)	0.29	0.78

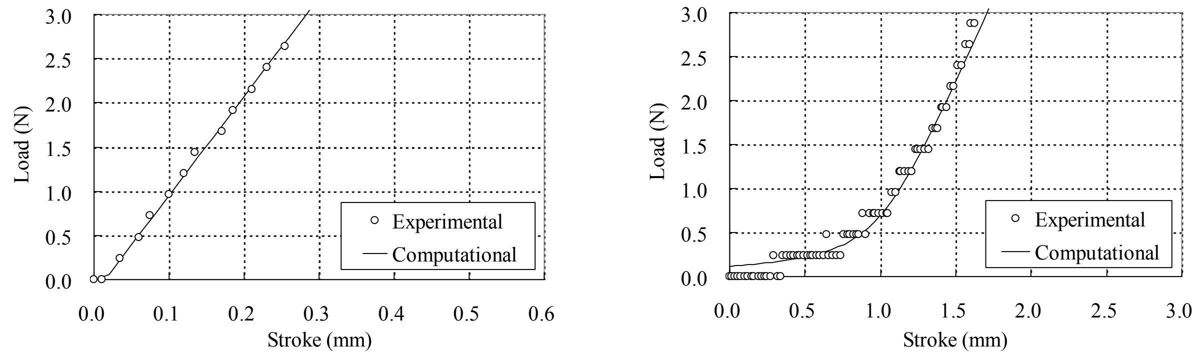

(a) Thin segment (b) Thick segment

Figure 6. Experimental and computational load-stroke relations

Table 2. Static loading cases

	Static Loads
S1	Self-weight
S2	Self-weight + Weight of a ball
S3	Self-weight + Concentrated load (in *Z*-dir.) on node 334

2.3 Static loadings

Nodal deflections under three cases of static loading are measured. In case S1, only self-weight is applied on the flexible net, and a ball, the weight of which is 5.174 N, is put on the center hexagonal unit of the net in case S2. In case S3, a *Z*-directional concentrated load is applied at the node 334 (see in Figure 3 (a)). The concentrated load is 1.862 N. The static load cases are listed in Table 2.

In the experiments, *Z*-directional nodal deflections from the initial horizontal plane (Z = 0) are measured by using a metal scale at the nodes along the sections A-A and B-B (along *X*- and *Y*-axes) in Figure 3 (a).

In the computational model, the net is discretized based on finite element method[13-15]. Let $\boldsymbol{u}$ denotes the vector of nodal displacements, and $\boldsymbol{R}(\boldsymbol{u})$ is defined as the internal nodal force vector. The external nodal force vector $\boldsymbol{F}(p)$ is given as a function of the load factor p. The vector of unbalanced nodal forces $\boldsymbol{E}(\boldsymbol{u}, p)$ is defined as difference between the internal and external nodal forces, and the equilibrium equation is written as

$$\boldsymbol{E}(\boldsymbol{u}, p) = \boldsymbol{R}(\boldsymbol{u}) - \boldsymbol{F}(p) = \boldsymbol{0} \tag{2}$$

In load case S1, the self-weight of the net is modeled as the constant nodal force vector $\boldsymbol{f}$. By substituting $\boldsymbol{F}(p) = \boldsymbol{f}$ for (2), the equilibrium equation under the state, where only self-weight is applied on the net, is given as follow.

$$\boldsymbol{E}(\boldsymbol{u}, p) = \boldsymbol{R}(\boldsymbol{u}) - \boldsymbol{f} = \boldsymbol{0} \tag{3}$$

$\boldsymbol{u}$ that satisfies equation (3) is found by Newton-Raphson Method.

In load cases S2 and S3, additional static load is written as $p\boldsymbol{e}$, where $\boldsymbol{e}$ denotes the mode of loading. From (2) and $\boldsymbol{F}(p) = \boldsymbol{f} + p\boldsymbol{e}$, the equilibrium equation in cases S2 and S3 is derived as

$$\boldsymbol{E}(\boldsymbol{u}, p) = \boldsymbol{R}(\boldsymbol{u}) - \boldsymbol{f} - p\boldsymbol{e} = \boldsymbol{0} \tag{4}$$

Load control method is applied for solving (4). In the computational process, the load factor p is increased, incrementally.

3 EXPERIMENTAL AND COMPUTATIONAL RESULTS

The nodal displacements in the equilibrium states of S1, S2 and S3 are shown in Figures 7 - 9, respectively. The blank circles and solid lines indicate the experimental and computational results. From Figures 7 (a) and (b), it is observed that the difference between experimental and computational results is sufficiently small. It is also confirmed that the equilibrium surface is smooth, and the hexagonal net resembles an isotropic membrane in structural behavior.

From Figures 8 (a) and (b), the large deflection is observed around the center of net. It can be also observed that the equilibrium surface is convex in the opposite direction to Figure 7. The nodal displacements by the computational analysis are close to those of experiment, but are slightly smaller than those of the experiment. It can be considered as the reason that one net segment is modeled as one finite element. The accuracy of analysis would be improved by discretizing one segment to several elements.

As shown in Figures 9 (a) and (b), remarkable local deformation can be seen in load case S3, and the equilibrium surface has a cusp at node 334. Also in this case, the nodal displacements are accurately obtained by the computational analysis.

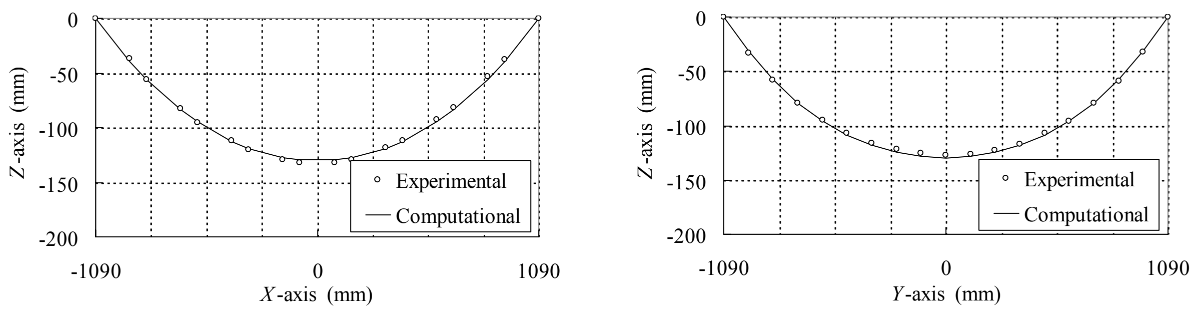

(a) Section A-A (b) Section B-B

Figure 7. Equilibrium surface in load case S1

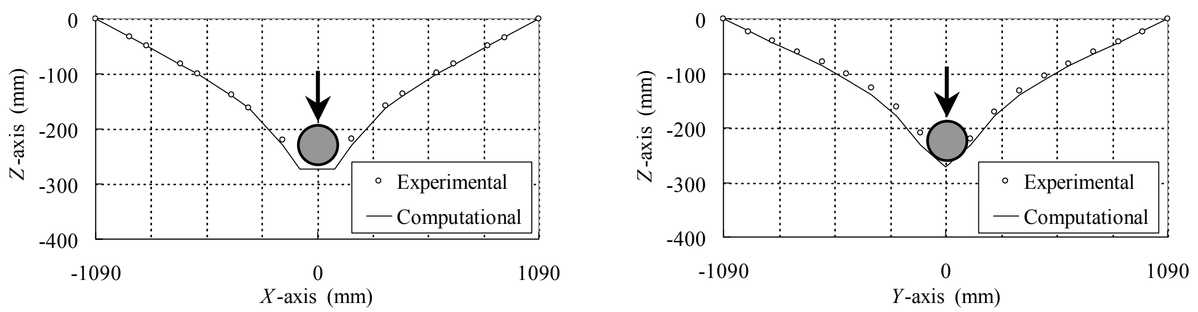

(a) Section A-A (b) Section B-B

Figure 8. Equilibrium surface in load case S2

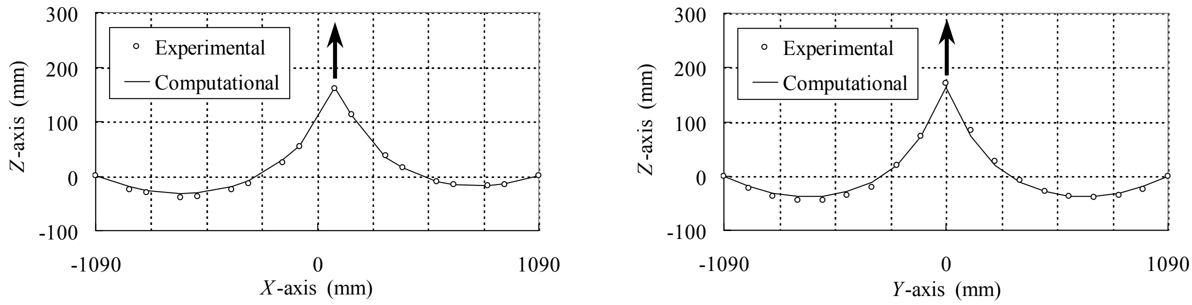

(a) Section A-A (b) Section B-B

Figure 9. Equilibrium surface in load case S3

From these results, it has been shown that the static behavior of the flexible nets can be accurately analyzed by using the proposed computational model.

4 CONCLUSIONS

Experimental and computational studies have been conducted for non- or low-prestressed nets (*flexible nets*). In the experiments, three cases of static loading have been applied to a flexible net, that has hexagonal units. The nodal displacements due to the static loads have been measured. Furthermore, a computational model for flexible nets has been proposed. The proposed computational model can represent static behavior of flexible nets, including stress-unilateral behavior. The constitutive parameters of proposed model have been determined based on tensile tests of the net segments. Numerical analyses have also been carried out under the same conditions as the static loading tests.

From the comparison between the experimental and computational results, it has been observed that the difference between the measured deflection and computed deflection is sufficiently small. It has been shown that the static behavior of the flexible nets under static loadings can be accurately analyzed by using the proposed computational model.

REFERENCE

[1] Architectural Institute of Japan, Guideline for Numerical Analysis of Spatial Structures, Architectural Institute of Japan, 2001. (in Japanese)
[2] Japan Society of Civil Engineering, Basis and Application of Cable and Space Structures, Japan Society of Civil Engineering, 1999. (in Japanese)
[3] Irvine HM, Sinclair GB, The suspended elastic cable under the action of concentrated vertical loads, Int. J. of Solids and Structures, 12, pp. 309-317, 1972.
[4] Leonard JW, Recher WW, Non-linear dynamics of cables with low initial tension, ASCE EM, 98, pp. 293-309, 1972.
[5] Leonard JW, Non-linear dynamics of cable elements, ASCE EM, 99, pp. 616-621, 1973.
[6] Piertzak J, Matrix formulation for static analysis of cable structures, Computers & Structures, 9, pp. 39-42, 1978.
[7] Leonard JW, Incremental response of 3-D cable network, ASCE EM, 99, pp. 621-629, 1973.
[8] Gambhir ML, Batchelor BV, A finite element for 3-D prestressed cable-nets, Int. J. of Num. Meth. Eng., Vol. 11, pp. 1699-1718, 1977.
[9] Fried I, Large deformation static and dynamic finite element analysis of extensible cables, Computers & Structures, Vol. 15, No. 3, pp. 315-319, 1982.
[10] Palkowski S, Statik der Seilkonstruktionen – Theorie und Zahlenbeispiele –, Springer-Verlag Berlin. 1990.
[11] Irvine M, Cable structures, Dover Publication Inc., New York, 1992.
[12] Broughton P, Nbumbaro P, The analysis of cable & catenary structures, Thomas Telford, 1994.
[13] Fujii F, Noguchi H, Osterrieder P, Static and dynamic large displacement response of flexible nets, IASS-APCS, Taipei, 2003.
[14] Fujii F, Noguchi H, Flexible nets in statics and dynamics, Proceedings Volume I, ISBN 951-39-1868-ECCOMAS2004, Jyvaskyla, Finland, CD-ROM, 2004.
[15] Fujii F, Noguchi H, K. Oda, Flexible and incompressive goal nets in soccer, Invited lecture, ICCM04, Singapore, 2004.